



## Free volume holes diffusion to describe physical aging in poly(methyl methacrylate)/silica nanocomposites

Daniele Cangialosi, Virginie M. Boucher, A. Alegría, and J. Colmenero

Citation: *J. Chem. Phys.* **135**, 014901 (2011); doi: 10.1063/1.3605600

View online: <http://dx.doi.org/10.1063/1.3605600>

View Table of Contents: <http://jcp.aip.org/resource/1/JCPSA6/v135/i1>

Published by the [American Institute of Physics](#).

---

### Related Articles

Influence of the adatom diffusion on selective growth of GaN nanowire regular arrays

*Appl. Phys. Lett.* **98**, 103102 (2011)

Hydrogenation of magnesium nanoblades: The effect of concentration dependent hydrogen diffusion

*Appl. Phys. Lett.* **98**, 081905 (2011)

Strong stress-enhanced diffusion in amorphous lithium alloy nanowire electrodes

*J. Appl. Phys.* **109**, 014310 (2011)

In situ microscopy of rapidly heated nano-Al and nano-Al/WO<sub>3</sub> thermites

*Appl. Phys. Lett.* **97**, 133104 (2010)

Transition from single-file to Fickian diffusion for binary mixtures in single-walled carbon nanotubes

*J. Chem. Phys.* **133**, 094501 (2010)

---

### Additional information on J. Chem. Phys.

Journal Homepage: <http://jcp.aip.org/>

Journal Information: [http://jcp.aip.org/about/about\\_the\\_journal](http://jcp.aip.org/about/about_the_journal)

Top downloads: [http://jcp.aip.org/features/most\\_downloaded](http://jcp.aip.org/features/most_downloaded)

Information for Authors: <http://jcp.aip.org/authors>

### ADVERTISEMENT

The logo for AIP Advances features the text 'AIP Advances' in a blue and green font. To the right of the text is a decorative graphic consisting of a series of orange circles of varying sizes, some of which are connected by a dotted line, suggesting a path or a network.

**AIP Advances**

*Submit Now*

**Explore AIP's new  
open-access journal**

- **Article-level metrics  
now available**
- **Join the conversation!  
Rate & comment on articles**

## Free volume holes diffusion to describe physical aging in poly(methyl methacrylate)/silica nanocomposites

Daniele Cangialosi,<sup>1,a)</sup> Virginie M. Boucher,<sup>2</sup> A. Alegría,<sup>1,3</sup> and J. Colmenero<sup>1,2,3</sup>

<sup>1</sup>Centro de Física de Materiales (CSIC-UPV/EHU), Paseo Manuel de Lardizabal 5, 20018 San Sebastián, Spain

<sup>2</sup>Donostia International Physics Center, Paseo Manuel de Lardizabal 4, 20018 San Sebastián, Spain

<sup>3</sup>Departamento de Física de Materiales, Universidad del País Vasco (UPV/EHU), Apartado 1072, 20080 San Sebastián, Spain

(Received 5 May 2011; accepted 8 June 2011; published online 1 July 2011)

The spontaneous thermodynamically driven densification, the so-called physical aging, of glassy poly(methyl methacrylate) (PMMA) and its nanocomposites with silica has been described by means of the free volume holes diffusion model. This mechanism is able to account for the partial decoupling between physical aging and segmental dynamics of PMMA in nanocomposites. The former has been found to be accelerated in PMMA/silica nanocomposites in comparison to “bulk” PMMA, whereas no difference between the segmental dynamics of bulk PMMA and that of the same polymer in nanocomposites has been observed. Thus, the rate of physical aging also depends on the amount of interface polymer/nanoparticles, where free volume holes disappear after diffusing through the polymer matrix. The free volume holes diffusion model is able to nicely capture the phenomenology of the physical aging process with a structure dependent diffusion coefficient. © 2011 American Institute of Physics. [doi:10.1063/1.3605600]

### I. INTRODUCTION

A liquid cooled down below the glass transition temperature ( $T_g$ ) undergoes slow spontaneous evolution towards the thermodynamic equilibrium characterized by an increase in the density. This process, known as physical aging, has been the subject of intense study since the pioneering investigation of Simon.<sup>1</sup> The phenomenology of physical aging was deeply investigated in glassy polymers by Kovacs<sup>2</sup> and Struik.<sup>3</sup> The common feature of these studies is that physical aging is intimately related to the molecular mobility of the polymer under examination.<sup>4</sup> To account for the change of the thermodynamic state during physical aging, the so-called nonlinearity is introduced in phenomenological models describing physical aging.<sup>5–7</sup> Despite the general success of these models in capturing the essential features of a large body of experimental results, the underlying mechanism of the physical aging process is still not fully understood.

Available theories<sup>8–10</sup> and a number of observations<sup>11,12</sup> mainly focus on the local nature of physical aging, but do not provide any explanation on the acceleration of physical aging recently encountered in thin films<sup>13–19</sup> and nanocomposites<sup>20–23</sup> when the typical size of the system (the thickness in thin films and the interparticle distance in nanocomposites) is of the order of (or lower) than several micrometers. In particular, Boucher *et al.*<sup>20,22</sup>—monitoring the evolution of the dielectric strength of PMMA secondary relaxation<sup>20</sup> and the enthalpy recovery<sup>22</sup> occurring during physical aging of poly(methylmethacrylate) (PMMA) in nanocomposites with silica particles displaying a diameter of the order of several hundreds of nanometers—observed

an acceleration of physical aging in the nanocomposites in comparison to bulk PMMA, whereas PMMA segmental dynamics—measured by broadband dielectric spectroscopy (BDS) that unequivocally probes spontaneous fluctuations in the glass former—was totally unaffected by the presence of silica nanoparticles. This means that, contrarily to the widely accepted view, in these systems physical aging and molecular mobility seem to be decoupled. Similar results have been found in other polymer nanocomposites.<sup>24</sup> Thus, the acceleration of physical aging in thin films and nanocomposites needs to be explained according to a mechanism that goes beyond a straightforward relationship between physical aging and molecular dynamics. Considering that the physical aging rate has been found to depend systematically on the amount of interfacial area per unit volume between the polymer and the nanoparticles, the diffusion of free volume holes from the polymer matrix to the interface could be invoked to explain the acceleration of physical aging. In this case, the acceleration of the physical aging process would be a natural consequence of the shorter distance free volume holes need to cover to reach the polymer interface.

The idea that the volume contraction generated by physical aging may be driven by free volume holes diffusion is not new and was first proposed long ago by Alfrey *et al.*<sup>25</sup> The diffusion mechanism was later questioned by Braun and Kovacs,<sup>26</sup> who found no differences in the physical aging rate between powdered and bulk polystyrene (PS). In this case, it is worth mentioning that the typical size of the powdered PS was of the order of tens of micrometers. The diffusion model was later revitalized by Curro *et al.*<sup>27</sup> A model conceptually analogous to that of Curro *et al.*,<sup>27</sup> based on the diffusion and annihilation of defects, was proposed and compared to experiments by Perez.<sup>28</sup> To account for the lack of sample-size

<sup>a)</sup>Electronic mail: swxcacad@sw.ehu.es.

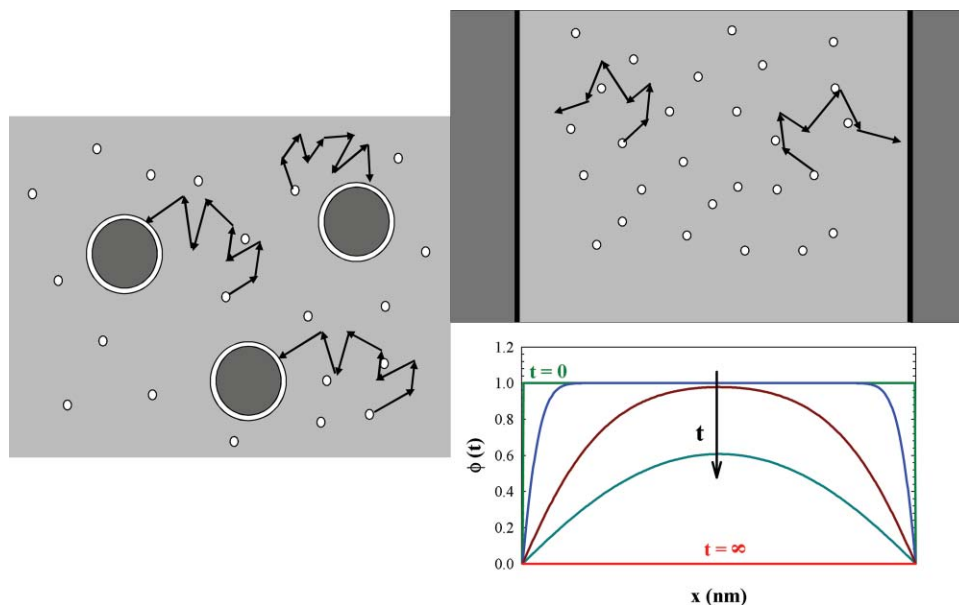


FIG. 1. Schematic illustration of the diffusion of free volume holes towards the interface: (a) in polymer nanocomposites; and (b) in the thin film equivalent to the nanocomposite (see text). Panel (c) represents the space distribution of a generic relaxation function in the thin film of panel (b).

dependence in the physical aging rate of bulk polymers, Curro *et al.*<sup>27</sup> assumed that an internal length scale for diffusion and annihilation of free volume holes exists. A length scale in the sub-micrometer range was assumed to achieve a physically meaningful diffusion coefficient for the volume recovery of poly(vinyl acetate) (PVAc). In the way it was developed, the model is able to capture most of the phenomenology of physical aging, namely, the description of up and down-jump experiments. As far as PVAc volume recovery experiments are concerned, memory effects are captured only in what concerns the time needed to reach the peak underlying these effects but not the amplitude.<sup>27</sup> These limitations suggest that other mechanisms may be relevant for the physical aging of “bulk” systems, whereas the diffusion mechanism is important when the typical length scale of the system is shorter than about 10  $\mu\text{m}$ .

More recently, the free volume holes diffusion model has been applied to the description of the accelerated physical aging of thin films of several glassy polymers.<sup>18,19,29,30</sup> In most cases, the diffusion equation was not resolved rigorously and different simplified approaches have been employed.<sup>18,19,30,31</sup> In the case of Ref. 29, the diffusion equation in combination with an other equation accounting for an additional mechanism, namely, lattice contraction, was resolved numerically.

In this work, we have applied the free volume holes diffusion model to previously published enthalpy relaxation data on PMMA/silica nanocomposites.<sup>21–23</sup> To do so, we have solved numerically the second equation of Fick with a free volume dependent diffusion coefficient. This was described by the Doolittle equation<sup>32</sup> that contains two adjustable parameters, namely, a reference diffusion coefficient ( $D_0$ ) and a structure and temperature independent parameter ( $B$ ). This approach was first applied to describe the enthalpy recovery of a set of PMMA/silica nanocomposites possessing a uniform distribution of non-aggregating nanoparticles<sup>20,22</sup> and, therefore, a well-defined ratio of area of silica to volume of

PMMA, having  $D_0$  and  $B$  as adjustable parameters. The second equation of Fick was subsequently applied to another set of PMMA/silica nanocomposites<sup>21,33</sup> displaying aggregation of the silica nanoparticles. In this case, the area of silica to volume of PMMA—being ill-defined due to the aforementioned aggregation—was the only adjustable parameter. In this case,  $D_0$  and  $B$  from the former set of PMMA/silica nanocomposites were employed as input parameters.

## II. FREE VOLUME DIFFUSION MODEL

The evolution of the thermodynamic state occurring in glassy polymers during physical aging below  $T_g$  is responsible for the change of all thermodynamic properties. Among them, the free volume, intimately related to the macroscopic volume, also decreases during physical aging. Within the free volume holes diffusion model such a decrease is described by the second equation of Fick,

$$\frac{\partial f_v(\vec{r}, t)}{\partial t} = \nabla(D\nabla f_v(\vec{r}, t)), \quad (1)$$

where  $f_v$  is the fractional free volume and  $D$  is the diffusion coefficient of free volume holes. Equation (1) implies that the driving force for physical aging is the free volume gradient. Equation (1) can be solved in two-dimensions exploiting the equivalence between nanocomposites and thin films.<sup>34</sup> In particular, from the point of view of the diffusion model, a nanocomposite can be approximated to a thin film when the following condition is fulfilled: the size of the nanoparticles is significantly larger than that of the free volume hole. This condition must be fulfilled because, to establish the equivalence with thin films, the surface of the nanoparticle has to be “seen” by the free volume hole reaching the interface as flat. In Fig. 1 the diffusion of free volume holes towards the interface between the nanoparticles and the polymer matrix (panel (a)) and the same process in the equivalent thin film

(panel (b)) are schematized. For the thin film Eq. (1) can be rewritten as

$$\frac{\partial f_v(x, t)}{\partial t} = \frac{\partial}{\partial x} \left( D \frac{\partial f_v(x, t)}{\partial x} \right), \quad (2)$$

where  $x$  is the dimension perpendicular to the surface of the thin film. The fractional free volume can be employed to define the relaxation function ( $\phi(x, t)$ ),

$$\phi(x, t) = \frac{f_v(x, t) - f_{v\infty}}{f_{v0} - f_{v\infty}} \quad (3)$$

that varies between 1—at the beginning of the aging process when the free volume is that obtained after quenching from above  $T_g$  to the selected aging temperature ( $f_v(x, t) = f_{v0}$ )—and 0—at the end of the aging process when the free volume has reached the equilibrium value ( $f_v(x, t) = f_{v\infty}$ ). In terms of the relaxation function, Eq. (2) can be rewritten as

$$\frac{\partial \phi(x, t)}{\partial t} = \frac{\partial}{\partial x} D \frac{\partial \phi(x, t)}{\partial x}. \quad (4)$$

To solve the second equation of Fick, it is necessary to define the boundary conditions, which in general depend on the thermo-mechanical history of the glass. In the case of aging experiments performed after quenching the glass from above  $T_g$  to the selected aging temperature, the two following boundary conditions can be introduced: (i) the free volume at the interface equals the relaxed value  $f_{v\infty}$  at any time during physical aging since, according to the diffusion model, in this position physical aging occurs instantaneously after the quench,

$$f_v(0, t) = f_{v\infty}, \quad f_v(s, t) = f_{v\infty} \quad t > 0 \quad (5)$$

and, according to Eq. (3),

$$\phi(0, t) = 0, \quad \phi(s, t) = 0 \quad t > 0, \quad (6)$$

where  $s$  is the thickness of the film; (ii) the free volume just after the quench to the selected aging temperature presents the unrelaxed value  $f_{v0}$  at any position except for the interface,

$$f_v(x, 0) = f_{v0}, \quad (7)$$

which for the relaxation function reads

$$\phi(x, 0) = 1. \quad (8)$$

An important ingredient that needs to be introduced in the diffusion model is the dependence of the diffusion coefficient on the thermodynamic state of the glass. This can be expressed according to the Doolittle equation<sup>32</sup>

$$D = D_0 \exp \left( \frac{B}{f_{v0}} - \frac{B}{f_v(x, t)} \right), \quad (9)$$

where  $D_0$  is the diffusion coefficient at a reference structure which is chosen to be that of the unrelaxed glass ( $f_v = f_{v0}$ ) and  $B$  is a material specific parameter. Equation (9) implies that, during the course of physical aging, the diffusion coefficient decreases quite dramatically making the systems increasingly sluggish. The Doolittle equation is conceptually analogous to the nonlinearity introduced in the more popular models describing physical aging.<sup>5-7</sup>

The application of the diffusion model requires the evaluation of the unrelaxed ( $f_{v0}$ ) and relaxed free volume ( $f_{v\infty}$ ). This can be done employing the Simha-Somcynski equation of state (EOS) theory,<sup>35</sup> which allows determining the free volume fraction once the specific volume is known. The theory can be written in terms of two coupled equations,

$$\frac{\tilde{P}\tilde{V}}{\tilde{T}} = [1 - 2^{-1/6}y(y\tilde{V})^{-1/3}]^{-1} + \frac{2y}{\tilde{T}}(y\tilde{V})^{-2}[1.011(y\tilde{V})^{-2} - 1.2045] \quad (10)$$

and

$$\begin{aligned} & \frac{s}{3c} \left[ \frac{s-1}{s} + y^{-1} \ln(1-y) \right] \\ &= \frac{y}{6\tilde{T}}(y\tilde{V})^{-2}[2.409 - 3.033(y\tilde{V})^{-2}] \\ &+ \left[ 2^{-1/6}y(y\tilde{V})^{-1/3} - \frac{1}{3} \right] [1 - 2^{-1/6}y(y\tilde{V})^{-1/3}]^{-1}, \end{aligned} \quad (11)$$

where  $\tilde{P} = P/P^*$ ,  $\tilde{V} = V/V^*$  ( $P^*$ ,  $V^*$ , and  $T^*$  being the scaling parameters depending on the Lennard-Jones interactions parameters; for details see Refs. 36 and 37) are the reduced  $PVT$  variables and  $y$  is the fraction of occupied volume, related to the free volume fraction through:  $f_v = 1 - y$ .  $P^*$ ,  $V^*$ , and  $T^*$  are the characteristic scaling parameters in MPa,  $\text{cm}^3/\text{g}$ , and K, respectively, that are determined from  $PVT$  equilibrium melt data and contain the molecular characteristics of the system. The flexibility ratio  $3c/s$ —where  $3c$  represents external volume dependent degrees of freedom and  $s$  is the number of segments in the polymer chain<sup>36-38</sup>—is generally assigned the value 1. The  $PVT$  variables were taken from the density measurements reported in Refs. 36 and 38.

In the present study, the fully relaxed  $f_{v\infty}$  and the unrelaxed  $f_{v0}$  free volume fractions have to be evaluated at the selected aging temperature. The former can be obtained simultaneously solving Eqs. (10) and (11) that deliver the equilibrium value of the free volume. Despite the Simha-Somcynski theory is generally developed for glass-formers in equilibrium, the unrelaxed free volume  $f_{v0}$  can still be obtained from the theory assuming that during the quench the free volume fraction remains constant. This implies that  $f_{v0}$  at the selected aging temperature equals the free volume fraction at the temperature from where the quench is performed.<sup>37,38</sup>

The solution of the free volume diffusion model with the introduction of the boundary conditions, the structure dependent diffusion coefficient through the Doolittle equation<sup>32</sup> and the free volume fraction from the Simha-Somcynski EOS theory<sup>35</sup> is displayed in Fig. 1 (panel (c)). In this figure, the spatial profile of the relaxation function in the thin film is displayed at several aging times. As expected, the free volume decreases faster close the interface and, for aging times different from  $t = 0$  and  $t = \infty$ , assumes a parabolic spatial profile.

Experimental data on physical aging are generally obtained as average quantities (e.g., the enthalpy of the

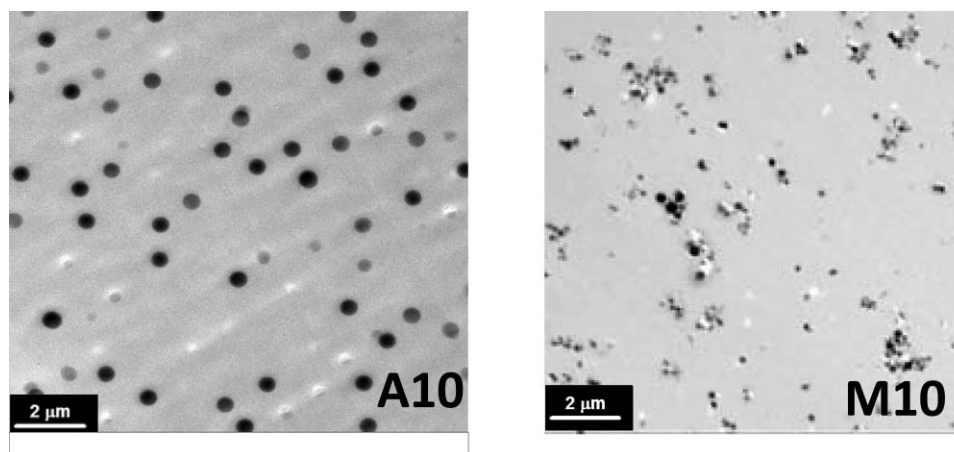


FIG. 2. Transmission electron micrograph images of a representative sample, where a homogeneous dispersion of the nanoparticles is achieved (A10) (Refs. 20 and 22) and one where aggregation of the nanoparticles is present (M10) (Refs. 21 and 33).

specimen). Thus, to compare the output of the diffusion model with experimental data, one has to perform a spatial averaging of the obtained magnitude. In the case of the relaxation function, the average is obtained as follows:

$$\bar{\phi}(t) = \frac{1}{s} \int_0^s \phi(x, t) dx. \quad (12)$$

To conclude this section, it is worth of remark that the so-developed diffusion model is rigorously applicable in nanostructured systems, where no specific interaction is present at the interface. In the case of the PMMA/silica nanocomposites, interactions are likely present at the interface between the polymer and silica nanoparticles. However, all systems object of our investigation, as will be seen later in the paper, display characteristic sizes larger than 100 nm. Thus, a layer of several nanometers in proximity of the polymer/nanoparticle interface only affects marginally the accuracy of our treatment.

### III. APPLICATION TO EXPERIMENTAL DATA

In this section of the paper, the diffusion model is applied to recent results on the enthalpy recovery at 353 K of PMMA in silica nanocomposites.<sup>21,22,33</sup> Alternatively other material variables, also displaying significant variation during physical aging, could be employed. For instance, the decrease of the dielectric strength of PMMA secondary relaxation process occurring during physical aging could be considered instead.<sup>20</sup> All nanocomposites present segmental dynamics identical to that of pure PMMA.<sup>21,22,33</sup> Preliminarily to the application of the model, the input parameters specific to PMMA need to be collected. Table I summarizes the parameters relevant to the application of the model. All data, except for  $P^*$ ,  $T^*$ ,  $V^*$ , and  $B$  that are material specific, are displayed at 353 K.

The diffusion equation (Eq. (2)) with a diffusion coefficient dependent on the structure according to the Doolittle equation (Eq. (9)), is highly nonlinear and not amenable to analytical solution. Therefore, we have solved Eq. (2) numerically employing a finite code element.<sup>39</sup> As the model is developed in a symmetrical two-dimensional geometry, the input parameter to the model is the thickness of the film equivalent to the nanocomposites, namely, the film with an area to

volume ratio equal to that of the nanocomposite. The dimension of the film will be addressed as *equivalent thickness* in the rest of the manuscript, corresponding to twice the inverse of the area to volume ratio of the nanocomposite.

The diffusion model was first applied to describe the enthalpy recovery of PMMA/silica nanocomposites displaying homogeneously dispersed silica nanoparticles.<sup>20,22</sup> In that case, nanocomposites were produced via methyl methacrylate (MMA) *in situ* polymerization in the presence of functionalized silica nanoparticles. Pure PMMA was also obtained through the same route as a reference. Details about the samples preparation are given in Refs. 20 and 22. As an example, a TEM image of one of these PMMA/silica nanocomposites is displayed in Fig. 2 (left panel). No indication of silica nanoparticles aggregation appears from the observation of the TEM micrographs. Thus, in this case, the area of silica to volume of polymer (equal to twice the inverse of the equivalent thickness) corresponds to the calculated one, according to simple geometric considerations. The details of PMMA/silica nanocomposites with homogeneous dispersion of nanoparticles are presented in Table II.

In Fig. 3, the relaxation functions associated with the enthalpy recovery data at 353 K taken from Ref. 22 are displayed for all nanocomposites (and the reference, pure PMMA) of Table II (data points). In this figure, the spatially averaged relaxation function associated with the enthalpy

TABLE I. Relevant parameters of PMMA at 353 K for the application of the diffusion model.  $V_0$  and  $V_\infty$  are, respectively, the unrelaxed and the relaxed specific volume.  $P^*$ ,  $T^*$ , and  $V^*$  are the scaling parameters only depending on the Lennard-Jones interactions parameters.

Simha Somcynski EOS input:	$P^*$ (bar)	1076.5	Refs. 36 and 38
	$T^*$ (K)	11319.7	Refs. 36 and 38
	$V^*$ (ml/g)	0.83	Refs. 36 and 38
	$V_0$ (ml/g)	0.875	Refs. 36 and 38
	$V_\infty$ (ml/g)	0.854	Refs. 36 and 38
Simha Somcynski EOS output:	$f_{v0}$	0.093	this work
	$f_{v\infty}$	0.072	this work
Doolittle parameters (fitted)	$D_0$ (cm <sup>2</sup> s <sup>-1</sup> )	$6 \times 10^{-14}$	this work
	$B$	0.715	this work

TABLE II. Relevant parameters of PMMA/silica nanocomposites (and pure PMMA of the same series) (Refs. 20 and 22) presenting a homogeneous dispersion of silica particles. Silica nanoparticles are modified with 3-(Trimethoxysilyl) Propyl Methacrylate (TPM) and Octadecyltrimethoxysilane (OTMS), respectively, for A10 and V10 samples and R10 sample. The external equivalent thickness corresponds to the one evaluated according to simple geometric considerations, whereas the equivalent thickness was evaluated through Eq. (14).

Sample	$M_w$ (g/mol)	Silica wt. %	Silica vol. %	Particle diameter (nm)	$s_{ext}$ (nm)	$s$ (nm)
PMMA	880 000	...	...	...	...	2000
R10	877 000	8.9	4.1	350	2845	1175
A10	760 000	8.9	4.1	350	2845	1175
V10	830 000	8.9	4.1	200	1625	900

recovery is presented. Analogously to the relaxation function of the free volume, this can be written as

$$\bar{\phi}_H(t) = \frac{H(t) - H_\infty}{H_0 - H_\infty}, \quad (13)$$

A first inspection of Fig. 3 reveals the shorter aging time needed for the decay of the relaxation function in nanocomposites in comparison to pure PMMA. Furthermore, nanocomposites with equal surface of silica to volume of PMMA ratios display very similar time evolution of the relaxation function. These results qualitatively support the diffusion of free volume holes model since this mechanism predicts an acceleration of the physical aging process depending exclusively on the area of silica to volume of PMMA ratio.

PMMA/silica nanocomposites relaxation data were fitted simultaneously to the diffusion model as described in Sec. II of the manuscript having  $D_0$  and  $B$  as adjustable parameters. A mean square error minimization procedure was employed. The equivalent thickness of the sample was evaluated as twice the inverse of the total of the area to volume ratio. The latter is the sum of the external area to volume ratio that can be easily determined from the concentration of nanoparticles, and

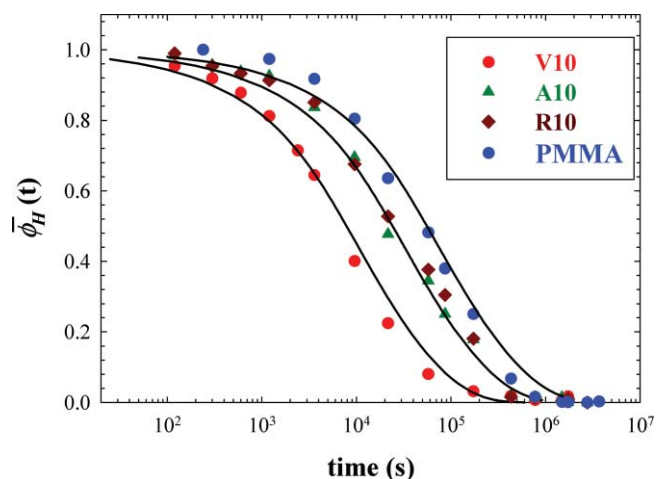


FIG. 3. Time evolution at 353 K of the relaxation functions determined from enthalpy recovery data of Ref. 22. The displayed data refer to the samples of Table II, namely, those displaying no aggregation of silica nanoparticles. The continuous lines are the fits to the diffusion model with  $D_0 = 6 \times 10^{-14}$  ( $\text{cm}^2 \text{s}^{-1}$ ) and  $B = 0.715$ .

the internal one, which corresponds to the intrinsic internal length scale of PMMA,<sup>27</sup> namely, that able to provide the fitting of pure PMMA recovery data. Thus the equivalent thickness can be calculated as follows:

$$s = \frac{s_{int}s_{ext}}{s_{ext} + s_{int}}, \quad (14)$$

where  $s_{int} = 2V/A_{int}$  and  $s_{ext} = 2V/A_{ext}$ . It is worth emphasizing that, while employed in our framework and proposed by several authors in the past,<sup>18,27,30,31</sup> the existence of an internal length scale is so far not proved though theorized by some authors.<sup>27,28</sup> Alternative approaches rather employ lattice contraction to account for the presence of physical aging also in bulk glasses.<sup>29</sup> In the latter case, the physical aging process for nanocomposites would result from the combination of the diffusion mechanism, relevant in highly confined systems, and that effective to equilibrate bulk systems. Contrarily the approach of the present work allows fitting all data with a single equilibration mechanism. Considering that the internal length scale is not known *a priori*, an iterative procedure was adopted to fit the data: (i) a first guess of the internal length was introduced and  $D_0$  and  $B$  obtained from the fit of the diffusion model to nanocomposites data; (ii) the so-obtained  $D_0$  and  $B$  were employed to fit recovery data for pure PMMA and a new value of the internal length scale was obtained; (iii) the latter value of the internal length scale was used to obtain the new value of  $D_0$  and  $B$  fitting data of the nanocomposites. This procedure allowed a rapid convergence to the best fit values of  $D_0$ ,  $B$ , and the internal length of pure PMMA.

The outputs of the fits are displayed in Fig. 3 as continuous lines. From the observation of the figure, one can clearly conclude that the diffusion model is able to quantitatively describe experimental data. Furthermore, the fitting parameters  $D_0$  and  $B$ , presented in Table I and in the caption of Fig. 3, are within the expected range of variation (Refs. 40 and 57). Thus, considering that the same set of  $D_0$  and  $B$  is able to fit the experimental data of all nanocomposites, the only parameter determining the rapidity of the enthalpy recovery is the equivalent thickness of the nanocomposite. In the case of pure PMMA, an equivalent thickness of 2000 nm was obtained, which is somewhat different from that estimated by Curro *et al.*,<sup>27</sup> when applying the diffusion model to the volume recovery of poly(vinyl acetate) (PVAc) (about 100 nm). However, in the work of Curro *et al.*,<sup>27</sup> the internal length scale was obtained assuming  $D_0 = 10^{-14} \text{ cm}^2 \text{ s}^{-1}$ . The latter value is chosen arbitrarily, whereas in the case of the present study the diffusion coefficient is that able to fit the physical aging data of nanocomposites, where the typical length scale is straightforwardly determined by the concentration and size of nanoparticles, once morphological analysis confirms a negligible level of aggregation of nanoparticles. Thus considering that an equivalent thickness in the micrometer range is expected for all polymers, we expect a larger diffusion coefficient for PVAc than that assumed by Curro *et al.*<sup>27</sup> The equivalent thickness obtained in the case of pure PMMA (2000 nm) allows rationalizing the similar aging rates observed in powdered and bulk PS,<sup>26</sup> since the former presents dimensions of the order of tens of micrometers.

TABLE III. Relevant parameters of PMMA/silica nanocomposites (and pure PMMA of the same series) (Refs. 21 and 33) presenting aggregation of silica particles. In all cases the particles diameter was 100 nm and the silica surface was modified with OTMS. PMMA molecular weight was:  $M_w = 120000$  g/mol and  $M_w/M_n = 1.1$ . The values of the equivalent thickness are obtained from the fitting of the diffusion model to the experimental data.

Sample	Silica wt. %	Silica vol. %	$s_{ext}$ (nm)	$s$ (nm)
PMMA	...	...	...	2000
M10	10	5	2880	1180
M17	17	8	1080	700
M24	24	12	470	380
M35	35	19	255	230
M52	52	32	185	170

Starting from the parameters  $D_0$  and  $B$  obtained fitting relaxation data of PMMA/silica nanocomposites listed in Table II, the diffusion model was extended to a set of enthalpy recovery experiments performed on PMMA/silica nanocomposites displaying aggregation of the silica nanoparticles but, at the same time, covering a wide range of silica concentrations. The details of these nanocomposites are displayed in Table III. In this case, PMMA/silica nanocomposites were prepared by solution casting. Details about the preparation of the sample are reported elsewhere.<sup>21,33</sup> The TEM of the sample labeled as M10 as an example, shown in Fig. 2 (right panel), clearly indicates that aggregation of silica nanoparticles occurs during the samples preparation.

Figure 4 presents the relaxation functions (data points) of all nanocomposites of the series of Table III included pure PMMA. A first inspection of the figure qualitatively indicates acceleration of the physical aging process in all nanocomposites in comparison to pure PMMA. Furthermore, the rate of physical aging clearly increases with the concentration of silica, i.e., with the area of silica to volume of PMMA ratio (twice the inverse of the equivalent thickness). Such acceleration is so marked in the nanocomposites with the largest silica concentration that the first recorded data already display a value of the relaxation function significantly lower than 1. This is due to the delay time, intrinsic to any experimental technique, that prevents the collection of data for aging times shorter than several minutes (depending on the experimental technique).

Before proceeding with the application of the diffusion model, it is worth comparing the relaxation function of pure PMMA of the series of Table III, with that of the pure polymer of Table II: the rapidity of enthalpy recovery is the same in the two PMMA samples, indicating that the physical aging process is not affected by the molecular weight, at least for the samples investigated in this work. This result is not surprising considering that the rate of PMMA physical aging does not depend on the molecular weight when this is larger than about  $M = 100000$  g/mol<sup>-1</sup> (Ref. 41). This result also agrees with the invariance of PMMA segmental dynamics for molecular weight larger than  $M = 100000$  g/mol<sup>-1</sup> (Ref. 42). This means that the parameters  $D_0$  and  $B$  employed for the previous series of nanocomposites are also representative of the molecular dynamics characteristics of PMMA of the second series of nanocomposites.

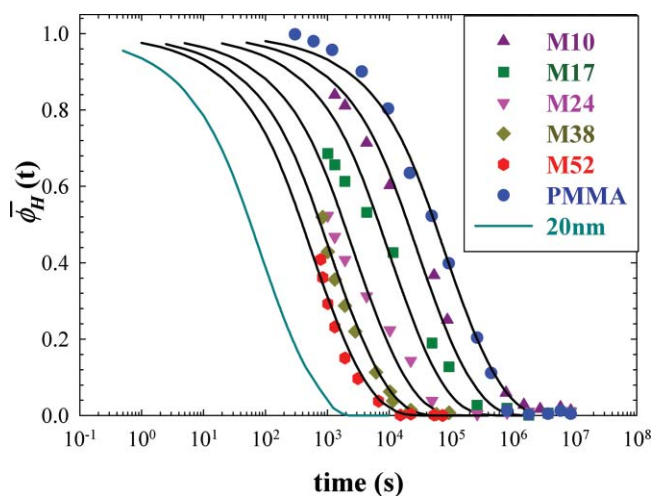


FIG. 4. Time evolution at 353 K of the relaxation functions determined from enthalpy recovery data of Ref. 21 and 33. The displayed data refer to the samples of Table III, namely, those displaying aggregation of silica nanoparticles. The continuous lines are the fits to the diffusion model with the equivalent thicknesses displayed in Table III. The parameters of the Doolittle equation were fixed at  $D_0 = 6 \times 10^{-14}$  cm<sup>2</sup> s<sup>-1</sup> and  $B = 0.715$  (see text). The (light) green continuous line is the prediction of the diffusion model for the enthalpy recovery of a 20 nm thick PMMA films undergoing physical aging at 353 K after quenching from above  $T_g$ .

The continuous lines in Fig. 4 represent the best description of experimental data through the diffusion model with the equivalent thickness of the nanocomposite as the only fitting parameter and  $D_0 = 6 \times 10^{-14}$  cm<sup>2</sup> s<sup>-1</sup> and  $B = 0.715$  as in the previous series of nanocomposites. As can be observed, the fit of enthalpy recovery data with equivalent thicknesses reported in Table III can be considered in all cases satisfactory. In some cases, the diffusion model predicts a somewhat less stretched time dependence of the enthalpy relaxation in comparison to experimental data. The origin of such a minor discrepancy may originate from the non-homogeneous distribution of silica nanoparticles (or aggregates as in this case) that is not accounted for by our simplified model.

As expected, the equivalent thicknesses obtained from the application of the diffusion model decrease with increasing the concentration of silica nanoparticles. To test quantitatively the physical significance of the obtained equivalent thicknesses, in Fig. 5 we have plotted the external area of silica to volume of polymer ratio ( $A_{ext}/V$ , corresponding to twice the inverse of the external equivalent thickness  $s_{ext}$ ) as a function of silica volume percentage. In the same figure, the calculated area to volume ratio, namely, that obtained assuming a homogeneous distribution of non-aggregating silica nanoparticles is displayed. The following considerations can be done from the observation of Fig. 5: (i)  $A_{ext}/V$  obtained from the diffusion model, similar to the calculated one, linearly scales with the silica volume percentage; (ii)  $A_{ext}/V$  from the diffusion model extrapolated from available data tends to zero at zero silica concentration. The former observation implies that the degree of aggregation is independent of the silica concentration. The latter indicates that the equivalent thicknesses obtained from the diffusion model are physically meaningful. A value of  $A_{ext}/V$  significantly different from zero at zero silica concentration would weaken

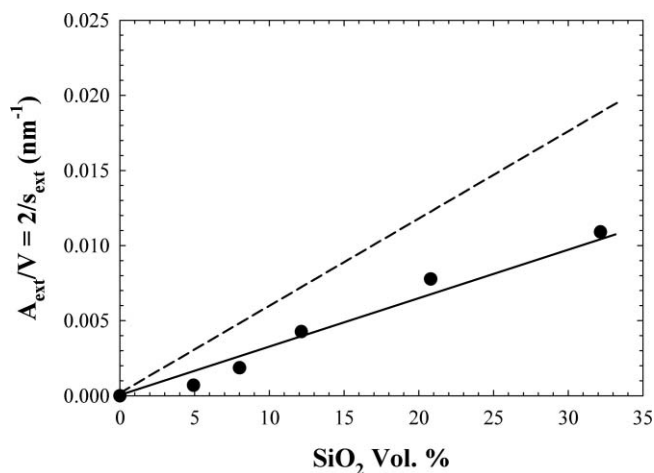


FIG. 5. External area of silica to volume of PMMA ratio versus silica volume percentage for PMMA/silica nanocomposites of Table III: determined by the diffusion model (closed circles and continuous line) and assuming a homogeneous dispersion of silica nanoparticles (dashed line).

the soundness of the diffusion model. Furthermore, the ratio between the  $A_{\text{ext}}/V$  calculated assuming a homogeneous distribution of non-aggregating silica nanoparticles and that found fitting data through the diffusion model is in all cases equal to 2. Such value, being larger than 1, is a measure of the degree of aggregation of silica particles.

To summarize this section, we have applied the diffusion model to describe the enthalpy recovery data of PMMA/silica nanocomposites displaying a wide range of area to volume ratios. The quality of the fits to the diffusion model is in all cases satisfactory and the fitting parameters physically sound. Thus, the diffusion of free volume holes is able to quantitatively capture the phenomenology of the physical aging process.

#### IV. DISCUSSION

In Sec. III of the paper, the application of the model consisting in the diffusion of free volume holes towards the interface between silica and PMMA was presented. Here, we discuss on the implications of the diffusion model and attempt to rationalize previously published physical aging data within the framework of such a model.

A straightforward implication of the diffusion model is that all experimental data, where acceleration of physical aging process is observed, can be conveniently described by such model. In particular, similar to the polymer nanocomposites investigated in this work,<sup>20–22,33</sup> the physical aging rate of polymer thin films with thickness in the range between several hundred nanometers and ten microns is enhanced in comparison to the corresponding bulk polymer.<sup>13–19,29</sup> A notable exception is represented by the work of Braun and Kovacs that reported no variation in comparison to the bulk of the rate of physical aging in powdered PS.<sup>26</sup> However, it is worth mentioning that in this case the typical size of the powdered PS was of the order of 10  $\mu\text{m}$  as evidenced by SEM micrographs. Moreover, the acceleration of the physical aging at confinement length scales larger than 100 nm is in

apparent contradiction with the ellipsometric results of Pye *et al.*<sup>43</sup> They found no variation of the rate of physical aging in PS films thicker than 100 nm in comparison to the bulk. In this case, the physical aging process is monitored in a time range of less than 2 orders of magnitude and with a time delay of about 10 min. Thus, the experimental data are likely representative of the region of most rapid variation of properties. All data about films thicker than 100 nm display the same slope, in agreement with our data that also present equal maximum slope (see Figs. 3 and 4).

In comparison to nanostructured materials with a confinement length scale larger than 100 nm, less trivial is the rationalization of aging experiments of thin films and polymer nanocomposites with a relatively large area to volume ratio, corresponding to an equivalent thickness shorter than several hundred nanometers. In this case, the vast majority of experimental works reports a reduction<sup>17,43–49</sup> or even a suppression<sup>45,50,51</sup> of physical aging.

This result apparently contrasts with the idea of free volume holes diffusion as the underlying mechanism for physical aging. Within the diffusion model, the reduction of the equivalent thickness of the nanostructured systems should induce a further acceleration of the physical aging process. However, it is worthy of remark that the scenario envisaged by the diffusion model implies a progressive increase of the rate of physical aging with decreasing the equivalent thickness of the system. This means that, according to the diffusion model, the time needed to stabilize the system at the selected aging temperature and to record the first data (the delay time) becomes inevitably too large in comparison with the time necessary for completion of the physical aging process. This is particularly crucial during the cooling process in the vicinity of (below) the  $T_g$  of the nanostructured glass, where significant densification of the system is expected to occur due to the combined effect of the large area to volume ratio and the relatively high temperature. This conjecture is corroborated by recent permeability experiments on polysulfone (PSF), which show that the permeability at the beginning of the aging process of the sub-100 nm thick films is considerably smaller than that of bulk PSF.<sup>17</sup> In the case of PMMA/silica nanocomposites reported in Table III, the value of the relaxation function recorded at the shortest aging time for which enthalpy recovery data can be achieved is always lower than the unity for all nanocomposites and increasingly smaller for nanocomposites with decreasing equivalent thicknesses. As thoroughly discussed in Ref. 33, the value of the relaxation function smaller than one is due to a lower initial enthalpy state rather than a different equilibrium state. The main consequence of the previous considerations is that nanostructured glasses possessing an equivalent thickness smaller than around 100 nm may display marginal or absent physical aging effects due to the completion of the process during the delay time, in particular during the cooling process, as previously discussed. Very recent experiments based on fast calorimetry on ultrathin glassy films (from 7 to 100 nm) clearly show for the first time acceleration of physical aging in ultrathin films. In this case, cooling rates larger than  $10^4 \text{ K s}^{-1}$  are achieved and; therefore, the significant densification occurring in proximity of  $T_g$  is considerably reduced.<sup>52</sup>



To quantitatively scrutinize this scenario, we have evaluated the expected behavior of the relaxation function at 353 K of a 20 nm thick PMMA film undergoing physical aging after quenching from above  $T_g$ . Such a function is displayed in Fig. 4 (light green continuous line). The Doolittle parameters,  $B$  and  $D_0$ , employed to simulate the relaxation function are the same as those obtained fitting experimental data. From the observation of the figure, one can conclude that for aging times of the order of several minutes—approximately equal to the typical delay time in aging experiments—the relaxation function decays almost completely. This implies that standard experimental techniques would not be able to provide any evolution of the monitored property after data acquisition begins. This may explain why in previously reported physical aging experiments on 20 nm thick PMMA films<sup>50</sup> no measurable effects on the monitored properties (the intensity of the fluorescent intensity) were observed. It is worthy of remark that in the case of Ref. 50, physical aging was monitored at  $T_{g,bulk} - 88 \text{ K} = 305 \text{ K}$ , a temperature somewhat lower than that employed to generate the time dependence of the relaxation function according to the diffusion model. Furthermore, the physical aging of 20 nm thick PMMA films may suffer of specific interactions with the substrate, given the non-negligible influence of a several nanometers thick dead layer.<sup>53–55</sup> Finally, one has to consider that the relaxation function of Fig. 4 has been generated imposing a perfect quench (infinite cooling rate) from above  $T_g$ , which is experimentally unachievable. This implies that a large part of the structural recovery may have already taken place during the cooling process, overall close to the  $T_g$  of PMMA. Notwithstanding the differences between the conditions employed to generate the relaxation function according to the diffusion model and those of Ref. 50, we have highlighted the possible influence of the inherent time delay in those experiments reporting reduced<sup>17,44–48</sup> or absent<sup>45,50,51</sup> physical aging effects. Therefore, we emphasize the need of rapid temperature stabilization setups<sup>52,56</sup> to provide evidence on the reliability of the scenario arising from the diffusion model in nanostructured systems with equivalent thicknesses shorter than several hundred nanometers.

An alternative proposed explanation to the reduction or suppression of physical in nanostructured PMMA/silica systems (Refs. 50 and 51) resides on the relatively strong hydrogen bond interaction between the polymer and silica. This would in turn reduce the mobility at the interface and; therefore, physical aging would be suppressed at such interface. Such a scenario has been also invoked in other nanostructured systems such as PVAc/silica<sup>48</sup> and layered silicate/epoxy<sup>46,47</sup> nanocomposites. The presence of a dead layer at the interface has been recently demonstrated.<sup>53–55</sup> However, this layer possesses a thickness of the order of several nanometers. In the case of the nanocomposites of the present study, the shortest equivalent thickness is of the order of 100 nm. Thus the presence of a dead layer, that accounts for about 1% of the total mass of polymer, is not able to rationalize the reduction of the recovered enthalpy in PMMA/silica nanocomposites listed in Table III. Furthermore, the reduction or suppression of physical aging has also been observed in weakly interacting nanostructured glasses,

such as *o*-terphenyl in a nanoporous matrix<sup>44</sup> and thin films of glassy PS (Ref. 45) and polymer membranes.<sup>17</sup> These observations pose serious concerns on the idea that physical aging is significantly reduced in those systems, where strong interaction with the interface is present, as far as molecular motion is not affected.

## V. CONCLUSIONS

The acceleration of physical aging observed in PMMA/silica nanocomposites in comparison to pure PMMA has been rationalized by means of the diffusion of free volume holes model. This is able to account for such acceleration without invoking any modification of the molecular mobility of the PMMA in the nanocomposites in comparison to the corresponding bulk system. PMMA dynamics is in fact unmodified by the presence of silica nanoparticles. Thus, the diffusion model allows rationalizing the partial decoupling between the physical aging and the molecular mobility of the glass, in the sense that the former is influenced by geometrical factors and not only by the latter. Enthalpy recovery data have been described by such model with a diffusion coefficient dependent on the structure according to the Doolittle equation. The so-formulated model allows to quantitatively describe enthalpy recovery data in the considered nanostructured systems. Finally, the implications on previously published results, in particular those reporting reduction or suppression of physical aging in several nanostructured glasses, have been discussed in the framework of the diffusion model.

## ACKNOWLEDGMENTS

The authors acknowledge the University of the Basque Country and Basque Country Government (Ref. No. IT-436-07, Depto. Educación, Universidades e Investigación) and Spanish Minister of Education (Grant Nos. MAT 2007-63681 and CSD2006-00053) for their support. The support of the Basque Government within the Eortek program is also acknowledged.

- <sup>1</sup>F. Simon, *Z. Anorg. Allg. Chem.* **203**, 219 (1931).
- <sup>2</sup>A. J. Kovacs, *Fortschr. Hochpolym.-Forsch.* **3**, 394 (1963).
- <sup>3</sup>L. C. E. Struik, *Physical Aging in Amorphous Glassy Polymers and Other Materials*, 1st ed. (Elsevier, Amsterdam, 1978).
- <sup>4</sup>J. Rault, *Physical Aging of Glasses* (Nova Science Publisher Inc., New York, 2009).
- <sup>5</sup>C. T. Moynihan, P. B. Macedo, C. J. Montrose, P. K. Gupta, M. A. D. Bolt, J. F. Dill, B. E. Dom, P. W. Drake, A. J. Easteal, P. B. Elterman, R. P. Moeller, H. Sasabe, and J. A. Wilder, *Ann. N. Y. Acad. Sci.* **279**, 15 (1976).
- <sup>6</sup>O. S. Narayanaswamy, *J. Am. Ceram. Soc.* **54**, 491 (1971).
- <sup>7</sup>A. J. Kovacs, J. J. Aklonis, J. M. Hutchinson, and A. R. Ramos, *J. Polym. Sci., Polym. Phys. Ed.* **17**, 1097 (1979).
- <sup>8</sup>V. Lubchenko and P. Wolynes, *J. Chem. Phys.* **121**, 2852 (2004).
- <sup>9</sup>G. Diezemann, *J. Chem. Phys.* **123**, 204510 (2005).
- <sup>10</sup>K. Chen and K. S. Schweizer, *Phys. Rev. E* **78**, 031802 (2008).
- <sup>11</sup>M. Arnoult, J. M. Saiter, C. Pareige, J. M. Meseguer Duenas, J. L. Gomez Ribelles, and J. Molina Mateo, *J. Chem. Phys.* **130**, 214905 (2009).
- <sup>12</sup>E. Schlosser and A. Schonhals, *Polymer* **32**, 2135 (1991).
- <sup>13</sup>P. H. Pfromm and W. J. Koros, *Polymer* **36**, 2379 (1995).
- <sup>14</sup>K. D. Dorkenoo and P. H. Pfromm, *Macromolecules* **33**, 3747 (2000).
- <sup>15</sup>M. S. McCaig and D. R. Paul, *Polymer* **41**, 629 (2000).

- <sup>16</sup>Y. Huang and D. R. Paul, *Macromolecules* **38**, 10148 (2005).
- <sup>17</sup>B. W. Rowe, B. D. Freeman, and D. R. Paul, *Polymer* **50**, 5565 (2009).
- <sup>18</sup>D. Cangialosi, M. Wubbenhorst, J. Groenewold, E. Mendes, H. Schut, A. van Veen, and S. J. Picken, *Phys. Rev. B* **70**, 224213 (2004).
- <sup>19</sup>D. Cangialosi, M. Wubbenhorst, J. Groenewold, E. Mendes, and S. J. Picken, *J. Non-Cryst. Solids* **351**, 2605 (2005).
- <sup>20</sup>V. M. Boucher, D. Cangialosi, A. Alegría, J. Colmenero, J. González-Irun, and L. M. Liz-Marzan, *Soft Matter* **6**, 3306 (2010).
- <sup>21</sup>V. M. Boucher, D. Cangialosi, A. Alegría, and J. Colmenero, *AIP Conf. Proc.* **1255**, 172 (2010).
- <sup>22</sup>V. M. Boucher, D. Cangialosi, A. Alegría, and J. Colmenero, *Macromolecules* **43**, 7594 (2010).
- <sup>23</sup>V. M. Boucher, D. Cangialosi, A. Alegría, and J. Colmenero, *J. Non-Cryst. Solids* **357**, 605609 (2011).
- <sup>24</sup>V. M. Boucher, D. Cangialosi, A. Alegría, J. Colmenero, I. Pastoriza-Santos, and L. M. Liz-Marzan, *Soft Matter* **7**, 3607 (2011).
- <sup>25</sup>T. Alfrey, G. Goldfinger, and H. Mark, *J. Appl. Phys.* **14**, 700 (1943).
- <sup>26</sup>G. Brown and A. J. Kovacs, *Phys. Chem. Glasses* **4**, 152 (1963).
- <sup>27</sup>J. G. Curro, R. R. Lagasse, and R. Simha, *Macromolecules* **15**, 1621 (1982).
- <sup>28</sup>J. Perez, *Polymer* **29**, 483 (1988).
- <sup>29</sup>M. S. McCaig, D. R. Paul, and J. W. Barlow, *Polymer* **41**, 639 (2000).
- <sup>30</sup>A. W. Thornton, K. M. Nairn, A. J. Hill, J. M. Hill, and Y. Huang, *J. Membr. Sci.* **338**, 38 (2009).
- <sup>31</sup>A. W. Thornton and A. J. Hill, *Ind. Eng. Chem. Res.* **49**, 12119 (2010).
- <sup>32</sup>A. K. Doolittle, *J. Appl. Phys.* **22**, 1471 (1951).
- <sup>33</sup>V. M. Boucher, D. Cangialosi, A. Alegría, and J. Colmenero, "Enhanced physical aging of polymer nanocomposites: the key role of the area to volume ratio," (unpublished).
- <sup>34</sup>A. Bansal, H. C. Yang, C. Z. Li, K. W. Cho, B. C. Benicewicz, S. K. Kumar, and L. S. Schadler, *Nature Mater.* **4**, 693 (2005).
- <sup>35</sup>R. Simha and T. Somchynski, *Macromolecules* **2**, 342 (1969).
- <sup>36</sup>L. A. Utracki and T. Sedlacek, *Rheol. Acta* **46**, 479 (2007).
- <sup>37</sup>L. A. Utracki, *Polym. Degrad. Stab.* **95**, 411 (2010).
- <sup>38</sup>M. Schmidt and F. H. J. Maurer, *Macromolecules* **33**, 3879 (2000).
- <sup>39</sup>S. Teukolsky, W. Vetterling, and B. Flannery, *Numerical Recipes in Fortran* (William Press, New York, 1996).
- <sup>40</sup>Values of  $B$  between 0.5 and 1 are generally quoted in literature (Ref. 57). The fitted value of  $D_0$  is consistent with that assumed by Curro *et al.* (Ref. 27).
- <sup>41</sup>L. Androzzi, M. Faetti, M. Giordano, and F. Zulli, *Macromolecules* **38**, 6056 (2005).
- <sup>42</sup>R. Casalini, C. M. Roland, and S. Capaccioli, *J. Chem. Phys.* **126**, 184903 (2007).
- <sup>43</sup>J. E. Pye, K. A. Rohald, E. A. Baker, and C. B. Roth, *Macromolecules* **43**, 8296 (2010).
- <sup>44</sup>S. L. Simon, J. Y. Park, and G. B. McKenna, *Eur. Phys. J. E* **8**, 209 (2002).
- <sup>45</sup>S. Kawana and R. A. L. Jones, *Eur. Phys. J. E* **10**, 223 (2003).
- <sup>46</sup>H. B. Lu and S. Nutt, *Macromolecules* **36**, 4010 (2003).
- <sup>47</sup>H. B. Lu and S. Nutt, *Macromol. Chem. Phys.* **204**, 1832 (2003).
- <sup>48</sup>S. Amanuel, A. N. Gaudette, and S. S. Sternstein, *J. Polym. Sci., Polym. Phys. Ed.* **46**, 2733 (2008).
- <sup>49</sup>Y. P. Koh and S. L. Simon, *J. Polym. Sci., Part B: Polym. Phys.* **46**, 2741 (2008).
- <sup>50</sup>R. D. Priestley, L. J. Broadbelt, and J. M. Torkelson, *Macromolecules* **38**, 654 (2005).
- <sup>51</sup>R. D. Priestley, P. Rittigstein, L. J. Broadbelt, K. Fukao, and J. M. Torkelson, *J. Phys.: Condens. Matter* **19** (2007).
- <sup>52</sup>A. Sepulveda, E. Leon-Gutierrez, and V.-R. J. Clavaguera-Mora M. T., "Accelerated aging in ultrathin films of a molecular glass former," *Phys. Rev. Lett* (in press).
- <sup>53</sup>D. Fragiadakis and P. Pissis, *J. Non-Cryst. Solids* **353**, 47 (2007).
- <sup>54</sup>A. Sargsyan, A. Tonoyan, S. Davtyan, and C. Schick, *Eur. Polym. J.* **43**, 3113 (2007).
- <sup>55</sup>S. E. Harton, S. K. Kumar, H. Yang, T. Koga, K. Hicks, E. Lee, J. Mijovic, M. Liu, R. S. Vallery, and D. W. Gidley, *Macromolecules* **43**, 3415 (2010).
- <sup>56</sup>B. Igarashi, T. Christensen, E. H. Larsen, N. B. Olsen, I. H. Pedersen, T. Rasmussen, and J. C. Dyre, *Rev. Sci. Instrum.* **79**, 045105 (2008).
- <sup>57</sup>R. A. Pethrick, *Prog. Polym. Sci.* **22**, 1 (1997).